

Signatures of mast cell activation are associated with severe COVID-19

Janessa Tan^{*1}, Danielle E. Anderson^{*1}, Abhay P. S. Rathore², Aled O'Neill¹, Chinmay Kumar Mantri¹, Wilfried A. A. Saron¹, Cheryl Lee³, Chu Wern Cui³, Adrian E. Z. Kang¹, Randy Foo¹, Shirin Kalimuddin^{1,4}, Jenny G. Low^{1,4}, Lena Ho^{3,5}, Paul Tambyah^{6,7}, Thomas W. Burke⁸, Christopher W. Woods^{8,9}, Kuan Rong Chan¹, Jörn Karhausen^{2,10}, Ashley L. St. John^{1,2,11,12**}

¹Program in Emerging Infectious Diseases, Duke-NUS Medical School, Singapore.

²Department of Pathology, Duke University Medical Center, Durham, NC, USA

³Duke-NUS Medical School, Program in Cardiovascular and Metabolic Disorders, Singapore

⁴Department of Infectious Diseases, Singapore General Hospital, Singapore

⁵Institute of Molecular and Cell Biology, A*STAR, Singapore

⁶Department of Medicine, Yong Loo Lin School of Medicine, National University of Singapore, Singapore

⁷Division of Infectious Disease, University Medicine Cluster, National University Hospital, Singapore

⁸Center for Applied Genomics and Precision Medicine, Duke University Medical Center, Durham, NC, USA.

⁹Division of Infectious Diseases, Duke University Medical Center; Durham VA Medical Center, Durham, NC, USA.

¹⁰Department of Anesthesiology, Duke University Medical Center

¹¹Department of Microbiology and Immunology, National University of Singapore, Singapore

¹²SingHealth Duke-NUS Global Health Institute, Singapore

*equal contribution

**correspondence: Ashley St. John, ashley.st.john@duke-nus.edu.sg

1 **Abstract**

2 Lung inflammation is a hallmark of Coronavirus disease 2019 (COVID-19) in severely ill patients and the
3 pathophysiology of disease is thought to be immune-mediated. Mast cells (MCs) are polyfunctional
4 immune cells present in the airways, where they respond to certain viruses and allergens, often
5 promoting inflammation. We observed widespread degranulation of MCs during acute and unresolved
6 airway inflammation in SARS-CoV-2-infected mice and non-human primates. In humans, transcriptional
7 changes in patients requiring oxygen supplementation also implicated cells with a MC phenotype. MC
8 activation in humans was confirmed, through detection of the MC-specific protease, chymase, levels of
9 which were significantly correlated with disease severity. These results support the association of MC
10 activation with severe COVID-19, suggesting potential strategies for intervention.

11

12

13 **Introduction**

14 Coronavirus Disease 2019 (COVID-19) is caused by Severe Acute Respiratory Syndrome Coronavirus 2
15 (SARS-CoV-2), a recently emerged coronavirus that has resulted in an ongoing global pandemic. Clinical
16 disease ranges from asymptomatic to mild to severe, and manifestations include upper respiratory tract
17 symptoms, pneumonia and, in some cases, acute respiratory distress syndrome (ARDS)(1). Fever, cough
18 and anosmia are most commonly experienced at disease presentation and complications involving the
19 vascular system can occur during severe disease(1). The lung is a major target organ of SARS-CoV-2
20 infection due to abundant expression of the angiotensin converting enzyme 2 (ACE2) receptor, a cellular
21 entry receptor for SARS-CoV-2(2). The virus is typically shed from the nasopharyngeal tract and
22 disseminated by coughing, but it can also be detected in fecal excretions(3). Various mouse and non-
23 human primate (NHP) models have been utilized to study COVID-19(4). Non-human primates (NHPs)
24 and human ACE2 (hACE2) knock-in mice both have been shown to experience infection and recapitulate
25 human signs of disease in the lung, including lung pathology(4). In human autopsy studies of severe
26 disease, infiltration of mononuclear cells in the lung tissue concurrent with edema and hemorrhage are
27 frequently described(5). It is believed that lung pathology during COVID-19 is immune-mediated and
28 compounded by the infiltration of monocytes, neutrophils and subsets of T cells(6). Interestingly,
29 perturbations in the numbers of granulocytes in the blood, such as neutrophils and eosinophils have also
30 been shown to be associated with severe disease(1, 7, 8).

31

32 Another granulocyte that responds to viral infections and is found in the lung tissue is the mast cell (MC).
33 MCs are long-lived granulated immune cells that are present in both connective and mucosal tissues(9).
34 In adults, MCs are thought to be derived from precursor cells circulating in the blood, known as MC
35 progenitors, but they are only found in mature form in tissues(10), making them difficult to study in
36 humans. Tissue resident MCs have a mature phenotype and express a variety of pathogen recognition
37 molecules on their surface and inside cytosolic compartments(11, 12). Their granules are loaded with pre-

38 formed mediators such as histamine, serotonin and unique MC-specific proteases, chymase and tryptase,
39 among others. Some of their mediators, including soluble cytokines and lipid mediators, may be also
40 produced by other granulocytes and immune cells(13). MC-derived products not only promote tissue
41 inflammation through the recruitment of cells such as monocytes, neutrophils and T cells, they also have
42 significant effects on vascular permeability and vasomotor control(9, 12, 14). The influence of MCs on
43 vasomotor control, including vasoconstriction and vasodilation, may also contribute to hypoxia that occurs
44 through shunting, which can influence vascular and tissue integrity(15). The tissue-specific
45 microenvironment where a MC resides influences its phenotype. For example, MCs in the atopic lung
46 express higher levels of IgE receptor, Fc ϵ R1 than in the skin(16, 17) and lung MCs are well characterized
47 to contribute to pathological lung inflammation during conditions such as asthma(18). MCs are known to
48 coordinate effective immune responses against invading pathogens, including viruses(12) but their
49 activation has also been linked to severe tissue damage, such as during dengue virus (DENV)
50 infection(19). In the lung, MC hyperplasia has also been reported during respiratory syncytial virus or
51 parainfluenza virus infections(20, 21) and therapeutic stabilization of MCs was shown to reduce lung
52 lesions in a model of highly pathogenic H5N1 influenza infection(22). However, sustained and systemic
53 activation of MCs could also result in severe pathologies such as coagulation disorders and vascular leak.
54 For example, MC-specific products such as chymase have been shown to be predictive of dengue
55 hemorrhagic fever and the severity of vascular leakage and coagulopathy that characterize severe
56 disease (19, 23, 24). MCs are present both in the nasal mucosae as well as in the deeper lung tissue
57 where SARS-CoV-2 infection occurs; however, it is unknown whether MCs respond to highly pathogenic
58 coronaviruses or if they could be involved in exacerbating the severe inflammation seen in SARS-CoV-2
59 infection.

60
61 In this study we aimed to assess MC activation in response to SARS-CoV-2 infection. Using mouse and
62 NHP models of COVID-19 we identified wide-spread MC degranulation in both acute and convalescent
63 lung tissues. In a human cohort, prospective analysis of the transcriptional signatures of MC-precursors
64 were highly enriched in the blood of patients who presented with severe COVID-19 disease, suggesting
65 modulation of this cell type during disease, as were several host response pathways for prominent MC-
66 derived products. Furthermore, the MC-specific product, chymase was significantly elevated in the sera of
67 SARS-CoV-2 infected patients confirming human MC activation during COVID-19 and supporting the
68 likelihood that MCs contribute to severe COVID-19 disease.

69
70 **Results and Discussion**
71
72 *MC degranulation coincides with lung pathology in animal models of COVID-19*
73

74 Given the association of MCs with chronic airway inflammation, their immune sentinel role for certain viral
75 pathogens, and knowing that severe lung inflammation also characterizes COVID-19, we first questioned
76 whether MCs are activated in animal models of SARS-CoV-2 infection. We used an established mouse
77 model where the receptor for SARS-CoV-2, hACE2, is delivered to the lungs using an adenovirus
78 vector(25). After hACE2-AAV inoculation, mice were infected with SARS-CoV-2 (**Fig. 1A**). Blood was
79 collected at multiple time points to assess MC-associated inflammatory products and tissues were
80 collected on days 5 and 7 post-infection for virus quantification by PCR. Mice showed the highest
81 infection burden in the lungs, but for at least some of the animals, SARS-CoV-2 could also be detected in
82 the spleen, liver, kidney, brain, and bone marrow (**Fig. 1B**), while the brachial lymph nodes were PCR-
83 negative at both time points (**Fig. S1**). Tissue histology revealed degranulation of MCs in the airways, as
84 shown in a representative image of the trachea at day 5 post-infection (**Fig. 1C**), where toluidine blue
85 staining of MC granules indicated extensive degranulation that coincided with edema in the tissue. In
86 contrast, granulated resting MCs can be observed in control trachea tissue (**Fig. 1C**). The trachea tissue
87 from control uninfected animals also appears healthy and compact, while the thickness of the trachea
88 tissue in SARS-CoV-2 infected animals appears increased as a result of inflammation and swelling (**Fig.**
89 **1C**). To provide a quantitation of MC activation, we also measured serum levels of the mouse chymase
90 MCPT1, which is a MC-specific protease that can be used as a biomarker of MC activation(19). MCPT1
91 levels were significantly elevated days 1, 3 and 5 post-SARS-CoV-2 infection and remained high, but
92 trending lower on day 7 (**Fig. 1D**), which we noted also coincided with reductions in viral burden in the
93 tissues (**Fig. 1B**). The evidence of MC degranulation in the airways combined with systemically elevated
94 MC products indicates that SARS-CoV-2 induces substantial activation of MCs during infection *in vivo*.
95

96 We next aimed to validate the MC activation phenotype in the non-human primate (NHP) model, which is
97 thought to more closely replicate the signs and symptoms of human SARS-CoV-2 infection(4). For this,
98 cynomolgus macaques were infected with 3×10^6 TCID-50 of SARS-CoV-2 virus intra-tracheally and they
99 were monitored with minimal interventions for 21 days prior to necropsy (**Fig. 2A**). Throughout the study
100 the animals were generally active, alert, and responsive. There were no significant changes in body
101 weight or temperature during the study (**Fig. S2**). Two NHPs (#6699 and 6727) displayed appetite loss,
102 and one was given subcutaneous fluids. SARS-CoV-2 could be detected in the nasal rinse or swab of all
103 NHPs at multiple time points during acute infection, as well as in the throat swab and lung lavage at least
104 one time point post-infection (**Fig. 2B**). Additionally, 3 of 4 NHPs were positive by rectal swab and 1 also
105 had detectable SARS-CoV-2 by eye swab (**Fig. 2B**). In support of active infection, all NHPs
106 seroconverted by day 14 (**Table S1**). At the time of necropsy on day 21, evidence of severe lung disease
107 was apparent, with all displaying damage to the lung tissue including areas of hemorrhaging visible on the
108 lungs and fluid accumulation in the lungs (**Fig. 2C-D**). Additionally, one NHP had blood clots inside the
109 lungs and 50% of NHPs had areas of black necrotic patches on the lungs (**Fig. 2C-D**), indicating severe
110 virus-induced pathology. RNA was extracted from lung tissue from each NHP and all samples were PCR-

111 negative for SARS-CoV-2. Interestingly, upon necropsy, NHP #6727 had detectable virus in the
112 cerebrospinal fluid (CSF). These findings suggested that the NHPs in this study experienced ongoing
113 inflammation and tissue damage even after the resolution of active infection.

114

115 Histological assessments of lung tissue showed severe damage to the airways and lung-associated
116 vasculature that coincided with activation of MCs in tissues. Signs of hemorrhage were present in the
117 lung tissue, where red blood cells (RBCs) were observed in the extravascular space, both trapped within
118 the alveoli, which were occasionally abnormally thickened (**Fig. 2E-F, S3**), as well as near blood vessels
119 (**Fig. 2G, S3**). Proximal to blood vessels there was also evidence of infiltration of immune cells into the
120 tissue (**Fig. 2G**) and fibrin deposition (**Fig. S3**). In multiple locations within the lung, including in the
121 trachea and the lower lung lobes, as well as near bronchi and near alveolar spaces, hypodense MCs
122 could be observed after staining of tissue sections with toluidine blue, suggesting their recent
123 degranulation (**Fig. 2H**). Free granules could be observed extracellularly near MCs (**Fig. 2H**), also
124 indicating degranulation. This widespread activation of MCs was confirmed by fluorescence staining to
125 detect heparin-containing granules in the lung tissue (**Fig. 2I-K**). We noted that activated MCs were
126 especially densely located and degranulating within the hemorrhagic regions of the infected lung tissue
127 (**Fig. 2H, J**). At higher magnification, free granules could be observed near hypogranulated MCs (**Fig.**
128 **2K**), also indicating recent degranulation. These results support that SARS-CoV-2 infected NHPs
129 experience lung pathology involving hemorrhagic manifestations and widespread MC activation, which
130 persists to late time points in the disease course.

131

132 *Signatures of MC transcriptional activation are associated with severe COVID-19*

133

134 In healthy humans, MC precursors make up a minor component of the blood, ~0.005% of cells(26). MCs
135 are known to have a unique transcriptional profile that clusters separately from other immune cells and
136 gene expression patterns have been identified that are either MC-specific or that typify both MCs and
137 basophils(27). Although MCs are not present in mature form in the blood, we considered that their
138 activation in peripheral tissues could influence the MC precursors or lead to transcriptional activation
139 profiles in immune cells that are consistent with responses to systemically elevated MC-associated
140 products. To investigate this, we examined whole blood transcriptomics data from a cohort of 4 mild and 6
141 severe COVID-19 patients, where clusters of genes that were temporally modulated during severe
142 disease progression and resolution were identified (28). Consenting patients were prospectively recruited
143 and were defined as severe on the basis of requiring supplemental oxygen during hospitalization. In the
144 patients with severe disease, the gene expression levels were monitored from -4 days to 13 days,
145 relative to the day when their condition peaked in severity of respiratory distress, which was defined as
146 time=0 (28). Interestingly, many genes associated with the MC lineage (**Fig. 3A-B**) or MC and also
147 basophil lineages (**Fig. 3C-D**) were differentially modulated in the blood of human COVID-19 patients with

148 severe disease (p-value < 0.05; q-value < 0.05; likelihood ratio test). Upregulation of several genes
149 associated with the MC- or MC/basophil transcriptional signature(27) occurred during the acute phase of
150 severe disease (**Fig. 3A,C**), while others were differentially regulated at the time of disease resolution
151 (**Fig. 3B,D**). The increased MC gene expression changes that were observed during the acute phase of
152 disease tracked tightly with respiratory function and resolved commensurate with respiratory improvement
153 (**Fig. 3E**). In contrast, these MC-associated transcripts were not collectively changed temporally
154 throughout the period of monitoring in mild COVID-19 presentation (**Fig S4A-E**), although some genes
155 that were associated with these signatures were still modulated, but to a lesser extent than in severe
156 patients (**Fig. S4A-D**). Pathway analysis of the temporally modulated genes over the disease course of
157 severely ill patients revealed significant perturbation of pathways downstream of key MC-associated
158 immune receptors (**Fig. 3F**) such as KIT (**Fig. 3G**), the receptor for stem cell factor, which is an important
159 stem cell-associated gene that is retained on MC precursors and mature MCs and regulates MC survival
160 and proliferation(29), and Fc ϵ RI (**Fig. 3H**), which is upregulated with MC maturation, although also
161 expressed by other cell types such as basophils(26, 27). These data show an enrichment of MC-
162 associated transcripts in patients with severe COVID-19 and support a potential role of MCs in shaping
163 disease severity.

164

165 *Confirmation of MC activation in human COVID-19 patients*

166

167 We next examined mild and severe COVID-19 patient blood for evidence that could indicate responses to
168 MC products and for biomarkers of MC activation. We noted that in addition to the significant modulation
169 of pathways associated with MC identity and maturation (**Fig. 3F-H**), pathway analysis of the whole blood
170 transcriptomics from severe patients also revealed significant modulation of pathways associated with
171 responses to well-established MC products (**Fig. 4A**). For example, Gap and adherens junction signaling,
172 which are influenced by MC proteases to promote vascular permeability(14), were activated, as was
173 signaling downstream of important, albeit not cell-specific, MC products, such as VEGF, TNF, Endothelin
174 1, and Eicosanoids (**Fig. 4A**). We also noted a significant influence on the renin-angiotensin pathway,
175 which is intriguing since chymase mediates angiotensin-converting enzyme (ACE)-independent
176 angiotensin II production (**Fig. 4A**).

177

178 To confirm the activation of MCs in humans, we also measured plasma chymase levels in two other
179 separate cohorts of COVID-19 patients. In the first cohort, the levels of plasma chymase were measured
180 in 13 patients that presented with mild disease and were treated as outpatients, (“community”), and
181 compared to the plasma chymase levels of 24 patients, in whom severe disease necessitated
182 hospitalization (“inpatients”), or to non-COVID-19 controls (**Fig. 4B**). The WHO 10-point median clinical
183 disease severity(30) in inpatients was 6 (25th and 75th interquartile, 5 and 7.25), including 7 intubated
184 patients and 3 patients with lethal outcomes. As non-COVID-19 controls we obtained baseline plasma

185 samples (after the induction of anesthesia, before incision) from patients who underwent coronary bypass
186 surgery. This cohort was chosen since they have many of the risk factors of COVID-19 patients and are of
187 a similar age. In both mild and severe COVID-19 cases, the plasma sample was collected at the time of
188 diagnosis for the majority of patients. These results indicated that hospitalized COVID-19 inpatients have
189 significantly higher levels of plasma chymase compared to community cases (**Fig. 4B**). This difference
190 was emphasized when the chymase levels in community cases were compared to hospitalized patients
191 that required intubation (**Fig. 4B**). Published reports highlight the importance of microvascular
192 abnormalities in defining COVID-19 severity(31) and are supported by the demonstration of alveolar
193 edema and hemorrhagic lesions in our murine and NHP models. MC activation has direct impact on
194 vascular function and integrity and, therefore, we tested if MC activation was linked to vascular barrier
195 dysfunction. For this, we measured Angiopoietin (Ang)-1 and -2 levels as markers of endothelial
196 activation, which are strongly linked with disease severity in ARDS(32) and COVID-19(32) and found no
197 change in Ang1 levels (**Fig. 4C**), yet higher Ang2 levels (**Fig. 4D**), resulting in higher Ang2/Ang1 ratios
198 (**Fig 4E**) in hospitalized and intubated vs. community COVID-19 cases. We also recruited a smaller
199 number of COVID-19 patients in Singapore. Indeed, this second cohort of COVID-19 patients also had
200 elevated chymase that was much higher than healthy controls and also averaged higher than the
201 concentrations detected in acute dengue patients (**Fig. S5**). These data were not stratified by severity due
202 to the smaller cohort size but support the activation of MCs in human COVID-19 patients. Taken together,
203 human chymase detection confirms that elevated chymase and heightened MC activation are associated
204 with severe COVID-19.
205

206 Our results indicate that MCs are strongly activated by SARS-CoV-2 infection *in vivo* in animal models,
207 and that their levels of activation are significantly associated with severe COVID-19 disease in humans.
208 The activation response involves a degranulation and release of MC-associated pre-formed mediators,
209 which was confirmed visually by imaging of tissue sections as well as quantitatively by detection of MC-
210 specific chymase in the serum. MCs are present in the lung tissue, even prior to birth, and they are
211 important for regulating lung tissue inflammation during homeostasis and disease(33). The heightened
212 levels of persistent activation of MCs that we detected through the acute phase of natural and
213 experimental SARS-CoV-2 infections are likely to be important for amplifying inflammation, which could
214 be detrimental to recovery from infection and return to tissue homeostasis following infection clearance. In
215 mouse and NHP lung tissue, MCs were observed to be strongly degranulating, and their increased
216 density and morphological appearance of activation was associated with areas of tissue damage
217 characterized by edema, hemorrhaging and necrosis. This is consistent with the role for MCs in mediating
218 inflammation and pathology in the lung that was suggested by mouse models of highly pathogenic
219 influenza(22, 34). The persistent activated state observed in the lungs of NHPs, with sustained evidence
220 of MC activation at the relatively late time point post-infection when samples were no longer PCR-positive
221 for virus detection, suggests that ongoing inflammation in the tissue may occur even after infection has

222 resolved systemically. The late phase activation of MCs subsequent to infection clearance and
223 establishment of a humoral adaptive immune response could suggest a role for MCs in the sustained
224 inflammatory response that limits disease resolution. Consistent with this, all NHPs seroconverted by 3
225 weeks post-SARS-CoV-2 infection and beginning as early as 1 week post-infection. Interestingly, IgGs
226 targeting various self-antigens including IFNs, phospholipids and cytokines, as well as heightened total
227 IgE levels have been detected in severe COVID-19 patients(35-38). MCs respond to antibodies in unique
228 ways when triggered by antigen/antibody immune complexes. Classically, known for its activation by
229 crosslinking of IgE-Fc ϵ RI in the presence of an antigen, MCs can also be activated by IgG immune
230 complexes owing to their surface expression of activating Fc γ Rs(39-41) . In addition to genes that are
231 consistent with a MC-specific transcriptional profile, we also found significant upregulation of pathways
232 typifying both MCs and basophils (27) in severe compared to mild COVID-19 patients, such as multiple Fc
233 receptors. Whether MCs can also be activated by autoantibodies that are evoked in the absence of an
234 active infection remains to be elucidated and might be relevant to long COVID-19 with persistent
235 symptoms.

236

237 We also observed transcriptional responses of severe COVID-19 patients that coincide with peak
238 respiratory distress and which point to the enhanced function or abundance of cells having a MC-like
239 phenotype. Pathways characteristic of pro-inflammatory responses of responder cells to MC-derived
240 products were also modulated. Since mature MCs are not present in the blood(10) and only present in
241 tissues, the MC associated phenotype described here is likely more consistent with MC precursors than
242 with mature MCs. We noted that transcripts of proteins that are specific to mature granulated MCs, such
243 as chymase, were not identified as a component of the MC-associated transcriptional profile that was
244 induced along the time course of peak severity. These results are highly suggestive of the expansion or
245 increased maturation of MC precursors in the blood, but further studies are needed to fully understand the
246 responses of this cellular compartment to infection. A limitation here is the potential to only monitor
247 transcriptional responses in the human blood, yet, our animal model data supports that there is expansion
248 of MCs in the lung tissue as well. This is consistent with the observation in a murine model of H1N1
249 influenza infection where recruitment and maturation of MC progenitors in the lung was suggested to
250 occur approximately 2 weeks after the infection(34). We also noted an unusually high density of MCs in
251 damaged and hemorrhagic regions NHP lungs at 3 weeks post SARS-CoV-2 infection. Increased
252 transcriptional upregulation of the chemokine CXCR2 in the blood of severe COVID human patients is
253 also suggestive of MC precursor migration into lung, as was seen in the context of other diseases(42).
254 Similarly, other studies have identified transcriptional signatures of granulocyte activation as well as
255 increases in cells such as neutrophils, eosinophils and basophils and T cells in the blood or lung tissue
256 itself in severe COVID-19(1, 6-8). As tissue-resident cells, MCs are considered sentinels and they can
257 promote the trafficking of many of these cell types into tissues during both allergic and infection-induced
258 inflammation(9, 12, 43).

259
260 Aside from the lung-associated pathologies of COVID-19, some individuals also experience other
261 hematological changes and cardiovascular events, including intra-vascular coagulation, endothelial
262 damage with ischemic complications, the development of rashes that could be accentuated by damaged
263 microvasculature, and increased incidence of myocardial infarction(1, 44). These effects on the
264 vasculature and cardiovascular system are also consistent with the effects of MCs in other sterile
265 inflammatory conditions. MCs line the blood vessels within tissues(14), which not only places them in a
266 location where they can directly exert their effects on the vasculature, but also where their mediators can
267 gain access to the blood. We observe that lung SARS-CoV-2 inoculation in mice and humans both results
268 in increased levels of MC-specific chymase, on a systemic level. In the renin-angiotensin system, MC-
269 chymase is a potent converter of angiotensin I to angiotensin II, which regulates microvascular blood flow
270 and systemic blood pressure(45-47). However, production of chymase by MCs is also associated with
271 vascular diseases. For example, in atherosclerotic aorta, angiotensin II activity was largely ACE-
272 independent and dependent on chymase(48) and increased expression of chymase in the lung was
273 associated with early pulmonary vascular disease(49). Notably, higher levels of angiotensin II in the
274 plasma of COVID-19 patients are correlated with lung injury suggesting its involvement in the tissue
275 damage(50). Moreover, angiotensin II could increase the expression of endothelial-specific receptor
276 tyrosine kinase (TIE2) ligand, Ang2(51). An imbalance of Ang2/1 is known to be associated with vascular
277 leakage and coagulation in other diseases(52). We observed increased plasma levels of Ang2 and
278 increased ratio of Ang2/Ang1 in severe COVID-19 patients compared to milder COVID-19 patients or
279 healthy controls. Interestingly, we also observed transcriptional responses of the angiotensin pathway
280 were substantially perturbed in the peripheral blood of severe COVID-19 patients. As exemplified by the
281 endothelial activation in severe COVID-19, this highlights a potential causal role of MC activation in
282 critical features of COVID-19 disease, including abnormalities of pulmonary blood flow leading to shunting
283 and hypoxemia or loss of endothelial integrity leading to tissue edema. Notwithstanding its role as an
284 angiotensin converting enzyme, a more direct effect of chymase in cleaving endothelial tight junctions or
285 potential contributions of other MC products, such as tryptase and serotonin(12), in COVID-19 related
286 vascular pathologies cannot be ruled out. As such, we found intriguing parallels to DENV as another virus
287 that induces MC activation. Although DENV does not specifically infect the lung, DENV infection is also
288 characterized by increases in microvascular permeability and bleeding, which are augmented through the
289 actions of MCs. It is noteworthy that in dengue, MCs play an important role in limiting virus burden in early
290 disease, but drive clinical deterioration in disseminated disease(12). As a result, drugs targeting MCs and
291 their products are promising as a therapeutic strategy to prevent severe clinical courses in DENV
292 infection and may bear similar promise in preventing severe COVID-19, which warrants further evaluation.
293

294 **Methods**

295

296 *Study approvals*

297 All mouse and primate studies were approved by the SingHealth Institutional Animal Care and Use
298 Committee of the SingHealth Experimental Medicine Centre (SEMC). The data associated with human
299 transcriptional responses was approved by the SingHealth Combined Institutional Review Board (CIRB
300 2017/2374). COVID-19 patients were recruited at Duke University in accordance with protocols reviewed
301 and approved by the Duke University Health System IRB (Pro00100241) while human COVID-19 patient
302 studies in Singapore were approved by the Domain Specific Review Board, Domain E for National
303 University Hospital (#2020/00120) and the National University of Singapore IRB (NUS-IRB-2021-186).

304

305 Additional Supplemental Methods accompany the study.

306

307 **Acknowledgments**

308 **Funding:** Duke-NUS Start-up funding to ALS; COVID19RF3-0033 to ALS and LH and National Medical
309 Research Council, Singapore COVID19RF2-0001 to DEA; R21, and NIH grants 1R21NS117973-01,
310 1R56HL126891-01, and a Duke School of Medicine Health Scholar Award to JK. **Authors contributions:**
311 JT, DA, APSR, AO, CKM, and WAAS performed experiments and data analyses. Data were interpreted
312 by JT, DA, APSR, KRC, JK and ALS. ALS and APSR wrote the manuscript with contributions by JT. The
313 primate study was designed, funded and conducted by DA with contributions from AEZK and RF.
314 Histological assessments in mice and primates were done by APSR. hACE2-AAV mouse model was
315 established and validated by CL, CWC and LH. Transcriptional analysis was performed by KRC with
316 additional interpretation by ALS. Human clinical sample collection and patient assessments were
317 performed by JL, SK, PT, TB and CW. Funding for the study was obtained by LH, JK, and ALS. The
318 project was conceived and supervised by ALS. All authors reviewed the manuscript and provided
319 feedback on it. **Competing interests:** The authors declare no competing interests. **Data and materials**
320 **availability:** All data needed to evaluate the conclusions in the paper are present in the paper and/or the
321 Supplementary Materials. Additional data related to this paper may be requested from the authors.

References

1. St John AL & Rathore APS (2020) Early Insights into Immune Responses during COVID-19. *J Immunol*.
2. Hoffmann M, et al. (2020) SARS-CoV-2 Cell Entry Depends on ACE2 and TMPRSS2 and Is Blocked by a Clinically Proven Protease Inhibitor. *Cell*.
3. Patel KP, et al. (2020) Transmission of SARS-CoV-2: an update of current literature. *Eur J Clin Microbiol Infect Dis* 39(11):2005-2011.
4. Munoz-Fontela C, et al. (2020) Animal models for COVID-19. *Nature* 586(7830):509-515.
5. Xu Z, et al. (2020) Pathological findings of COVID-19 associated with acute respiratory distress syndrome. *Lancet Respir Med* 8(4):420-422.
6. Song JW, et al. (2020) Immunological and inflammatory profiles in mild and severe cases of COVID-19. *Nat Commun* 11(1):3410.
7. Zhang JJ, et al. (2020) Clinical characteristics of 140 patients infected with SARS-CoV-2 in Wuhan, China. *Allergy* 75(7):1730-1741.
8. Vitte J, et al. (2020) A Granulocytic Signature Identifies COVID-19 and Its Severity. *J Infect Dis* 222(12):1985-1996.
9. Abraham SN & St John AL (2010) Mast cell-orchestrated immunity to pathogens. *Nat Rev Immunol* 10(6):440-452.
10. Ribatti D & Crivellato E (2014) Mast cell ontogeny: an historical overview. *Immunol Lett* 159(1-2):11-14.
11. St John AL & Abraham SN (2013) Innate immunity and its regulation by mast cells. *J Immunol* 190(9):4458-4463.
12. Rathore AP & St John AL (2020) Protective and pathogenic roles for mast cells during viral infections. *Curr Opin Immunol* 66:74-81.
13. Wernersson S & Pejler G (2014) Mast cell secretory granules: armed for battle. *Nat Rev Immunol* 14(7):478-494.
14. Kunder CA, St John AL, & Abraham SN (2011) Mast cell modulation of the vascular and lymphatic endothelium. *Blood*.
15. Nielsen HB (2003) Arterial desaturation during exercise in man: implication for O₂ uptake and work capacity. *Scand J Med Sci Sports* 13(6):339-358.
16. Andersson CK, et al. (2011) Alveolar mast cells shift to an FcepsilonRI-expressing phenotype in mild atopic asthma: a novel feature in allergic asthma pathology. *Allergy* 66(12):1590-1597.
17. Fujisawa D, et al. (2014) Expression of Mas-related gene X2 on mast cells is upregulated in the skin of patients with severe chronic urticaria. *J Allergy Clin Immunol* 134(3):622-633 e629.
18. Brown JM, Wilson TM, & Metcalfe DD (2008) The mast cell and allergic diseases: role in pathogenesis and implications for therapy. *Clin Exp Allergy* 38(1):4-18.
19. St John AL, Rathore AP, Raghavan B, Ng ML, & Abraham SN (2013) Contributions of mast cells and vasoactive products, leukotrienes and chymase, to dengue virus-induced vascular leakage. *eLife* 2:e00481.
20. Sorden SD & Castleman WL (1995) Virus-induced increases in bronchiolar mast cells in Brown Norway rats are associated with both local mast cell proliferation and increases in blood mast cell precursors. *Lab Invest* 73(2):197-204.
21. Castleman WL, Sorkness RL, Lemanske RF, Jr., & McAllister PK (1990) Viral bronchiolitis during early life induces increased numbers of bronchiolar mast cells and airway hyperresponsiveness. *Am J Pathol* 137(4):821-831.
22. Han D, et al. (2016) The therapeutic effects of sodium cromoglycate against influenza A virus H5N1 in mice. *Influenza Other Respir Viruses* 10(1):57-66.
23. St John AL & Rathore APS (2019) Adaptive immune responses to primary and secondary dengue virus infections. *Nat Rev Immunol* 19(4):218-230.
24. Tissera H, et al. (2017) Chymase is a Predictive Biomarker of Dengue Hemorrhagic Fever in Pediatric and Adult Patients. *J Infect Dis*.
25. Israelow B, et al. (2020) Mouse model of SARS-CoV-2 reveals inflammatory role of type I interferon signaling. *J Exp Med* 217(12).

26. Dahlin JS, et al. (2016) Lin- CD34hi CD117int/hi FcepsilonRI+ cells in human blood constitute a rare population of mast cell progenitors. *Blood* 127(4):383-391.
27. Dwyer DF, Barrett NA, Austen KF, & Immunological Genome Project C (2016) Expression profiling of constitutive mast cells reveals a unique identity within the immune system. *Nat Immunol* 17(7):878-887.
28. Ong EZ, Kalimuddin, S., Chia, W.C., Ooi, S.H., Koh, C.W.T., Tan, H.C., Zhang, S.L., Low, J.G., Ooi, E.E., Chan, K.R. (in press) Temporal dynamics of the host molecular responses underlying severe COVID-19 progression and disease resolution. *Ebiomedicine*.
29. Galli SJ, Tsai M, & Wershil BK (1993) The c-kit receptor, stem cell factor, and mast cells. What each is teaching us about the others. *Am J Pathol* 142(4):965-974.
30. Characterisation WHOWGOTC & Management of C-i (2020) A minimal common outcome measure set for COVID-19 clinical research. *Lancet Infect Dis* 20(8):e192-e197.
31. Ackermann M, et al. (2020) Pulmonary Vascular Endothelialitis, Thrombosis, and Angiogenesis in Covid-19. *N Engl J Med* 383(2):120-128.
32. Gutbier B, et al. (2018) Prognostic and Pathogenic Role of Angiopoietin-1 and -2 in Pneumonia. *Am J Respir Crit Care Med* 198(2):220-231.
33. Msallam R, et al. (2020) Fetal mast cells mediate postnatal allergic responses dependent on maternal IgE. *Science* 370(6519):941-950.
34. Zarnegar B, et al. (2017) Influenza Infection in Mice Induces Accumulation of Lung Mast Cells through the Recruitment and Maturation of Mast Cell Progenitors. *Front Immunol* 8:310.
35. Lucas C, et al. (2020) Longitudinal analyses reveal immunological misfiring in severe COVID-19. *Nature* 584(7821):463-469.
36. Bastard P, et al. (2020) Autoantibodies against type I IFNs in patients with life-threatening COVID-19. *Science* 370(6515).
37. Zuo Y, et al. (2020) Prothrombotic autoantibodies in serum from patients hospitalized with COVID-19. *Sci Transl Med* 12(570).
38. Wang EY, et al. (2020) Diverse Functional Autoantibodies in Patients with COVID-19. *medRxiv*.
39. Hazenbos WL, et al. (1996) Impaired IgG-dependent anaphylaxis and Arthus reaction in Fc gamma RIII (CD16) deficient mice. *Immunity* 5(2):181-188.
40. Miyajima I, et al. (1997) Systemic anaphylaxis in the mouse can be mediated largely through IgG1 and Fc gammaRIII. Assessment of the cardiopulmonary changes, mast cell degranulation, and death associated with active or IgE- or IgG1-dependent passive anaphylaxis. *J Clin Invest* 99(5):901-914.
41. Syenina A, Jagaraj CJ, Aman SA, Sridharan A, & St John AL (2015) Dengue vascular leakage is augmented by mast cell degranulation mediated by immunoglobulin Fcgamma receptors. *Elife* 4.
42. Hallgren J, et al. (2007) Pulmonary CXCR2 regulates VCAM-1 and antigen-induced recruitment of mast cell progenitors. *Proc Natl Acad Sci U S A* 104(51):20478-20483.
43. Galdiero MR, et al. (2017) Bidirectional Mast Cell-Eosinophil Interactions in Inflammatory Disorders and Cancer. *Front Med (Lausanne)* 4:103.
44. Modin D, et al. (2020) Acute COVID-19 and the Incidence of Ischemic Stroke and Acute Myocardial Infarction. *Circulation* 142(21):2080-2082.
45. Li M, et al. (2004) Involvement of chymase-mediated angiotensin II generation in blood pressure regulation. *J Clin Invest* 114(1):112-120.
46. Miyazaki M, Takai S, Jin D, & Muramatsu M (2006) Pathological roles of angiotensin II produced by mast cell chymase and the effects of chymase inhibition in animal models. *Pharmacol Ther* 112(3):668-676.
47. Fyhrquist F & Saijonmaa O (2008) Renin-angiotensin system revisited. *J Intern Med* 264(3):224-236.
48. Ihara M, et al. (1999) Increased chymase-dependent angiotensin II formation in human atherosclerotic aorta. *Hypertension* 33(6):1399-1405.
49. Hamada H, et al. (1999) Increased expression of mast cell chymase in the lungs of patients with congenital heart disease associated with early pulmonary vascular disease. *Am J Respir Crit Care Med* 160(4):1303-1308.
50. Liu Y, et al. (2020) Clinical and biochemical indexes from 2019-nCoV infected patients linked to viral loads and lung injury. *Sci China Life Sci* 63(3):364-374.
51. Otani A, Takagi H, Oh H, Koyama S, & Honda Y (2001) Angiotensin II induces expression of the Tie2 receptor ligand, angiopoietin-2, in bovine retinal endothelial cells. *Diabetes* 50(4):867-875.

52. Parikh SM (2016) Targeting Tie2 and the host vascular response in sepsis. *Sci Transl Med* 8(335):335fs339.

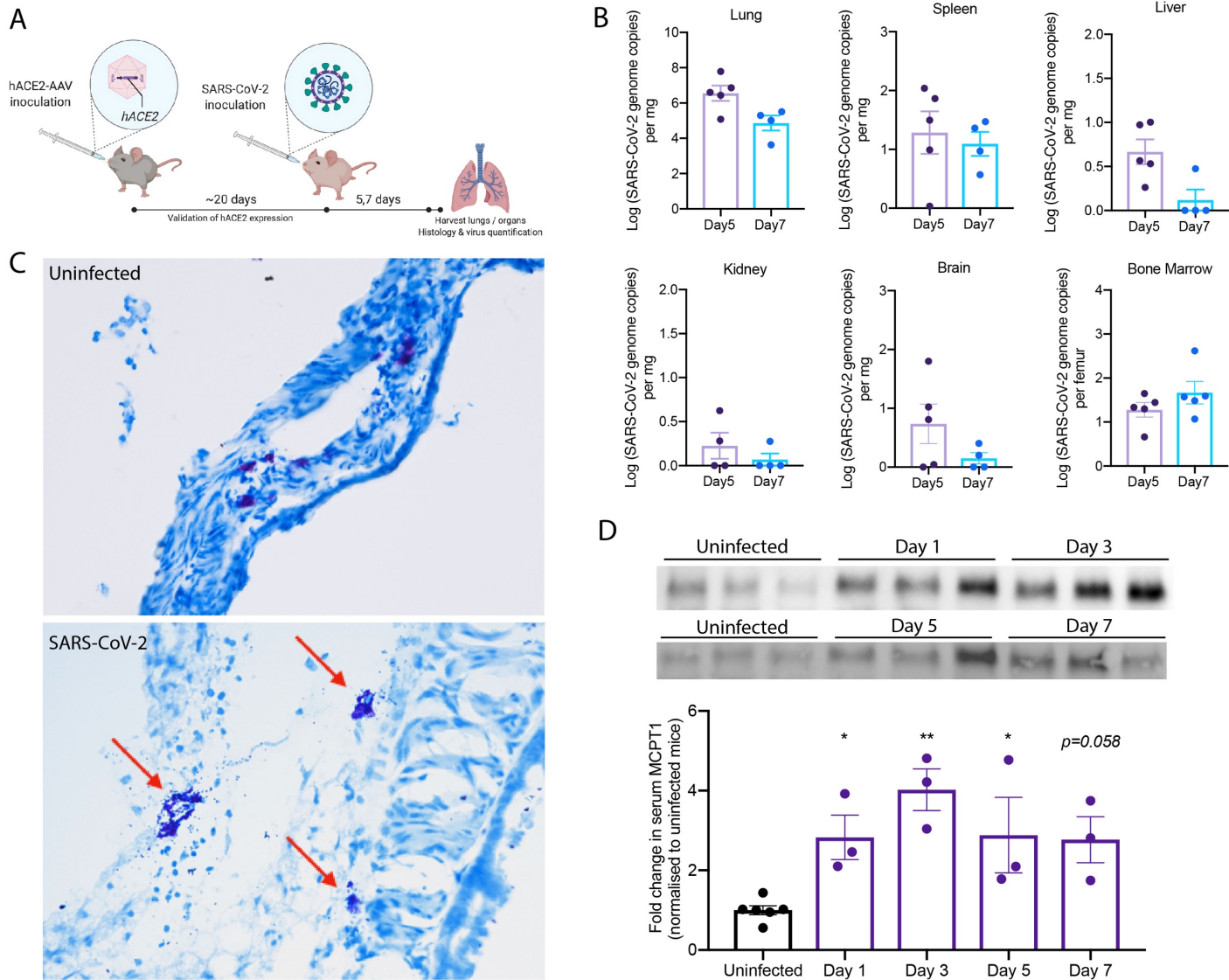


Figure 1. Degranulation of MCs in SARS-CoV-2 infected mice. (A) C57BL/6 mice were inoculated intranasally with *hACE2-AAV* to induce *hACE2* expression in the airways. SARS-CoV-2 (2×10^7 TCID₅₀) TCID-50) was inoculated intranasally into *hACE2-AAV* C57BL/6 mice. Blood was taken on days 1, 3, 5, and 7, and organs were harvested after 5 or 7 days for histology and virus quantification. (B) Virus quantification from the organs harvested shows detection in the lung, spleen, liver, kidney, brain, and bone marrow both Days 5 and 7. (C) Histology images of toluidine blue-stained trachea sections from uninfected and SARS-CoV-2 infected mice. Degranulating MCs (red arrow) could be observed in SARS-CoV-2 infected mice as well as tissue edema and airway narrowing. (D) Western blot images after chymase detection in serum Days 3, 5 and 7 post-infection shows systemic elevation of chymase, which was quantitated by densitometry from 3 individual mouse samples and presented as fold-increase over uninfected controls. Error bars represent the SEM. Chymase was significantly elevated in serum of infected mice compared to uninfected controls, determined by 1-way ANOVA with Dunnett's post-test; *p<0.05, **p<0.01. Non-significant p-values below p=0.01 are shown on the graph.

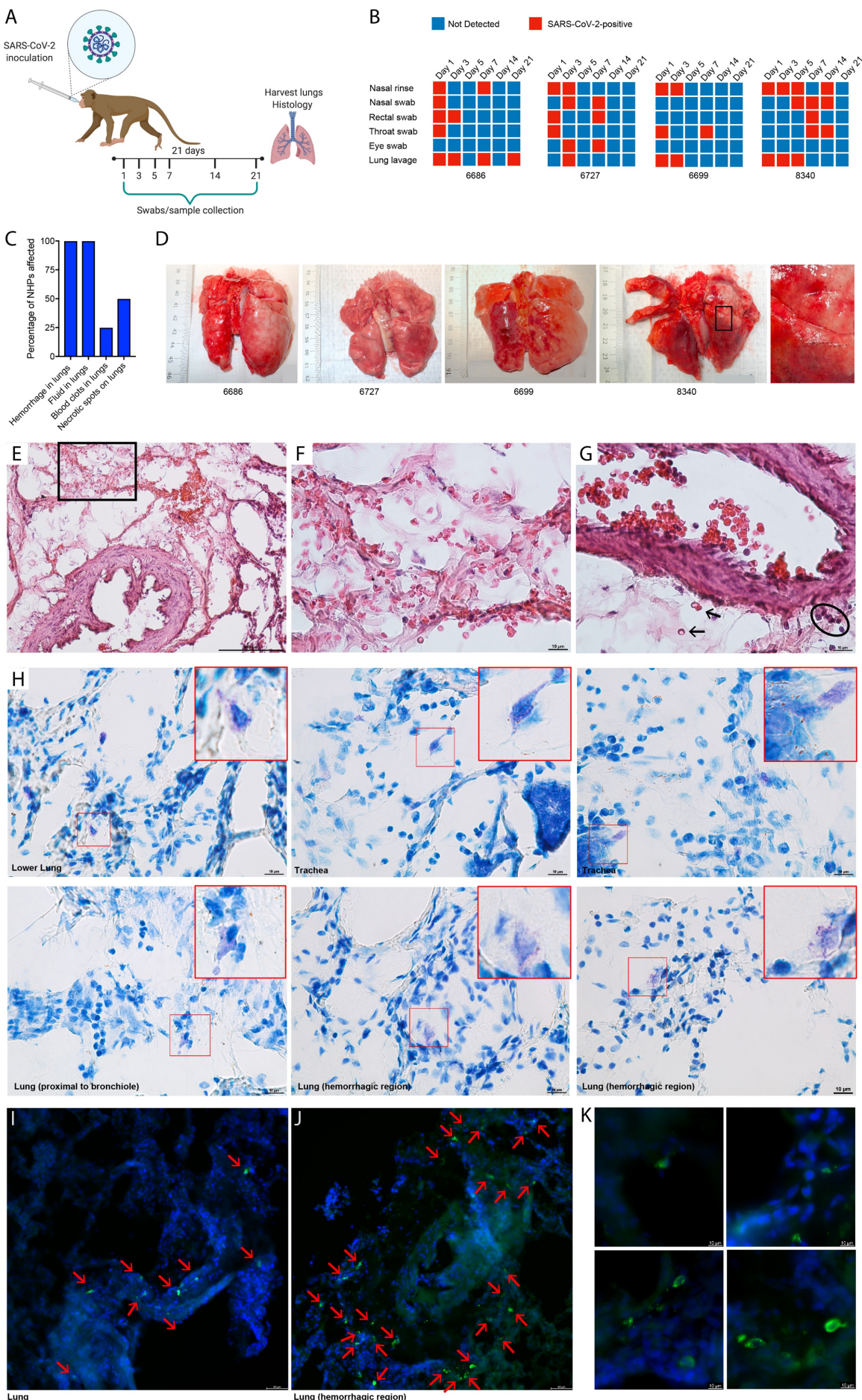


Figure 2. Widespread activation of MCs coinciding with lung pathology in NHPs. **(A)** Cynomolgus macaques were infected intratracheally with SARS-CoV-2 and monitored for 21 days prior to necropsy. **(B)** Viral detection was determined by PCR at regular intervals post-infection in swabs from multiple mucosal tissues, lung lavage, and nasal rinses. All NHPs were positive for SARS-CoV-2 infection multiple days after inoculation. **(C)** Abnormal findings related to lung tissue observed at the time of necropsy were recorded and effected all animals. **(D)** Images of NHP lungs at the time of necropsy show areas of hemorrhaging and necrotic spots on the lung surface. Boxed region is enlarged. **(E)** Histological assessment of lung tissues by H&E staining shows hemorrhaging of the tissue and free RBCs within the lung alveolar spaces. **(F)** Inset corresponding to the boxed region of panel H. **(G)** Some RBCs in the tissue proximal to a blood vessel are indicated by arrows and cellular infiltrates are circled. **(H)** Multiple examples of degranulating or hypogranulated MCs are provided, observed in toluidine blue stained lung tissue sections. The MCs are enlarged in the red-outlined insets. For **(I-K)**, lung sections were stained for MC heparin to indicate the location of MC granules (green) and DAPI to identify cellular nuclei and tissue structures. MCs are indicated with red arrows. **(I)** MCs were observed degranulating in the lung of SARS-CoV-2 infected primates in sections of a biopsy of lung tissue that did not have overt hemorrhaging visible on the lung surface at necropsy. **(J)** MCs appear more densely packed in the lung biopsy from a hemorrhagic lobe of the lung and again, degranulation is observed based on staining for MC-heparin. **(K)** Images of degranulating MCs are presented at higher magnification.

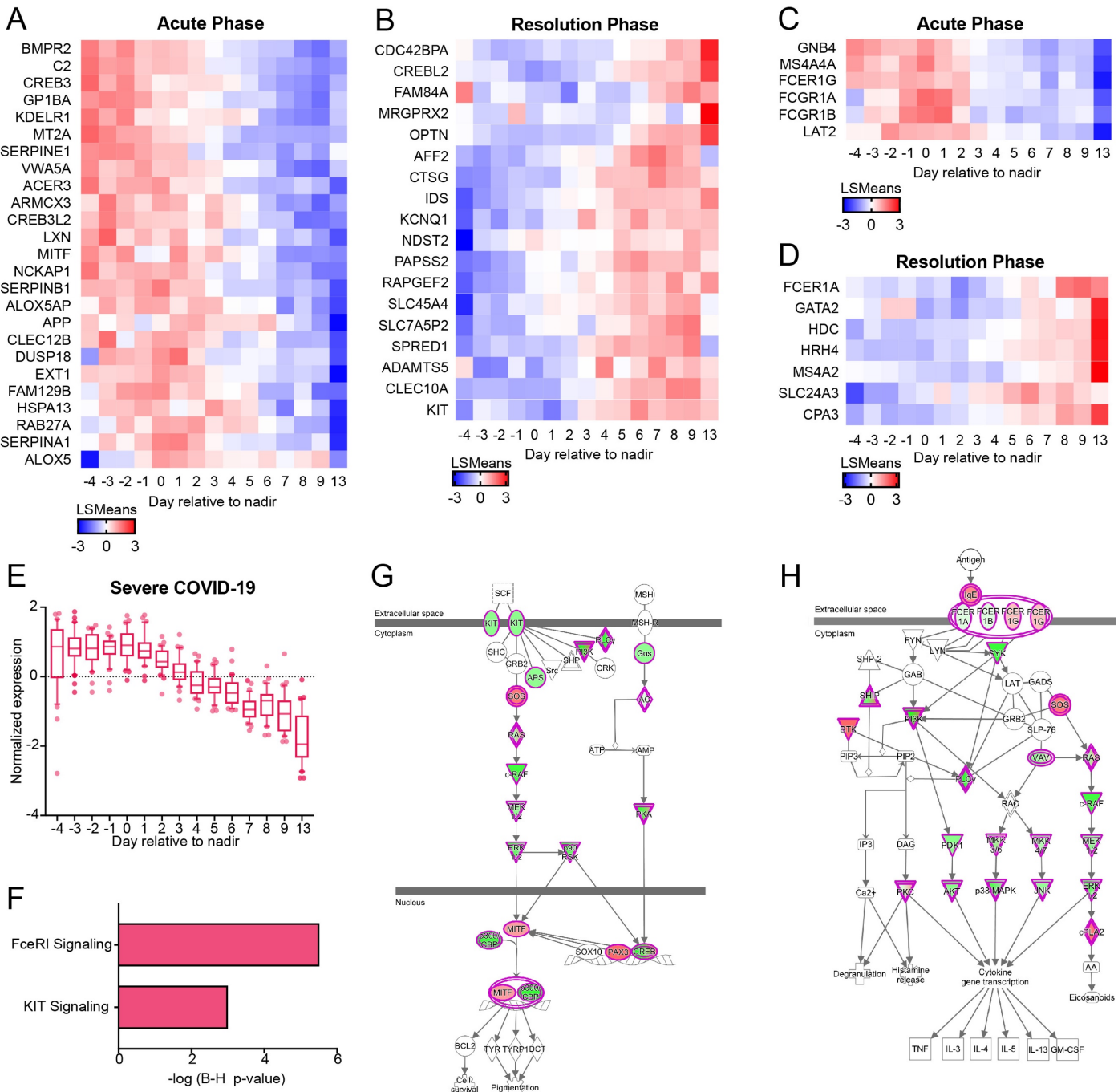


Figure 3: Transcriptional signatures of MC associated genes with severe COVID-19. Genes associated with a (A-B) MC-specific or (C-D) MC/basophil phenotype that were significantly regulated in PBMCs of severe COVID-19 patients. Heatmap shows the LSmean expression values of MC-specific or MC/basophil phenotype genes in severe COVID-19 patients ($n=6$) at the various days relative to the peak severity with respect to respiratory function (day 0). Clusters of genes that were significantly upregulated during the acute phase (A, C) or resolution phase (B, D) are presented. (E) Normalized expression levels of the MC-specific genes shown in A and C over time, in the severe COVID-19 patients. (F) Pathway analysis indicates a significant perturbation of pathways associated with MC function and/or MC-precursor maturation. Gene network analysis for the significantly modulated pathways (G) KIT and (H) Fc ϵ RI are shown. Red indicates the genes with increased expression during the acute phase, whereas green indicate genes with increased expression during the resolution phase.

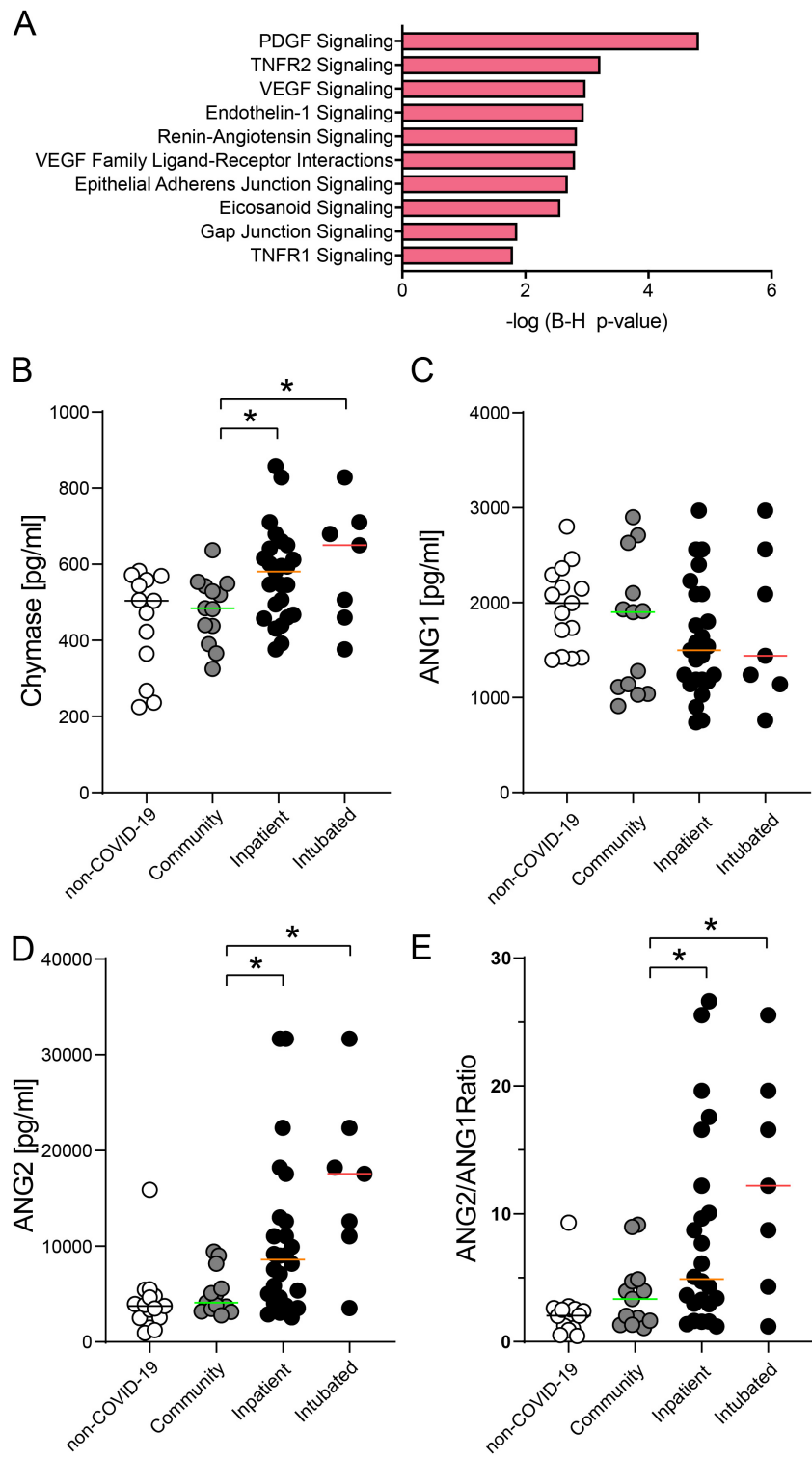


Figure 4: MC products and activation pathways associated with severe COVID-19. (A) Pathway analysis indicates a significant perturbation of pathways associated with host-responses to characteristic MC products. (B) Plasma chymase levels are increased in hospitalized patients “inpatient” compared to mild “community” patients and in intubated patients compared to mild patients. (C) No significant changes in ANG1 levels in inpatient and intubated patients compared to community cases and non-COVID-19 controls. (D) Significantly increased plasma ANG2 levels and (E) ANG2/ANG1 ratios in inpatients compared to community patients. One-way ANOVA was performed and considered significant for post-test p-values <0.05. For panels, **B-E**, non-COVID-19 patients n=12-15; For community, n=13; for inpatients n=24; n=7.